Chapter 3: Hydrogenolysis of [PhB(CH_2PPh_2)$_3$]Fe≡N-*p*-tolyl: Probing the Reactivity of an Iron Imide with H_2

The text in this chapter is reproduced in part with permission from:

Brown, S. D.; Peters, J. C. *J. Am. Chem. Soc.* **2004,** *126,* 4538.

Copyright 2004 American Chemical Society

3.1 Introduction

It is generally accepted that low-coordinate iron nitride species are formed and hydrogenated on the surface of solid-state iron catalysts in the Haber-Bosch process.[1] Moreover, it has been postulated that Fe-N (and/or Mo-N) multiple bonds may be formed from N_2 and further reduced by hydrogen equivalents (i.e., H^+/e^-) during turnover in nitrogenase enzymes.[2] Studying the reactivity patterns of hydrogen with molecular iron complexes featuring Fe-N multiple bond linkages is therefore of considerable interest but has been difficult to undertake due to the historical absence of well-defined Fe=NR and/or Fe≡N species.[3]

Our group has recently reported the synthesis of a number of mononuclear imides of iron and cobalt (e.g., $[PhBP^R_3]M(NR)$ where $[PhBP^R_3]$ = $[PhB(CH_2PPh_2)_3]^-$ and $[PhB(CH_2P^iPr_2)_3]^-$).[4] These trivalent imides are characterized by relatively robust M≡NR triple bonds ($1\sigma + 2\pi$) but are nonetheless able to release their imide functionalities, an example being transfer to CO producing isocyanate.[4a,b] This group-transfer reactivity prompted us to survey their respective reactivities toward hydrogen.

3.2 Results and Discussion

The low-spin cobalt complex $[PhBP_3]Co{\equiv}N$-*p*-tolyl[4b] is stable to hydrogen pressure (1-3 atm) at modest temperatures (≤70 °C). By contrast, low-spin $[PhBP_3]Fe{\equiv}N$-*p*-tolyl (**2.5**)[4a] gives rise to a fascinating reaction profile upon exposure to 1 atm of H_2 at room temperature. Both partial and complete hydrogenolysis of the Fe≡NR linkage is observed. Whereas H_2-promoted reduction of an imide to its corresponding amide was first described by Wolczanski,[5] reductive scission of a metal imide by hydrogen to release amine has not to our knowledge been previously reported.[6]

Fingerprint resonances for imide **2.5** are conveniently monitored by ^{1}H NMR spectroscopy despite its paramagnetic S = ½ ground state.[4a] When a sealable NMR tube is charged with forest green **2.5** in C_6D_6 under an atmosphere of H_2, its resonances fully decay within a period of 3 h at room temperature. During this time, the reaction solution remains homogeneous, and the color changes to an intense red/purple. The major reaction product at this stage is the paramagnetic anilido complex [$PhBP_3$]Fe(N(H)-*p*-tolyl) (**3.1**) (Equation 3.1).[7] Assignment of **3.1** from its paramagnetically shifted ^{1}H NMR resonances is aided by comparison to a spectrum of an independently generated sample of **3.1** prepared by the reaction between [Li][N(H)-*p*-tolyl] and [$PhBP_3$]FeCl.[4a]

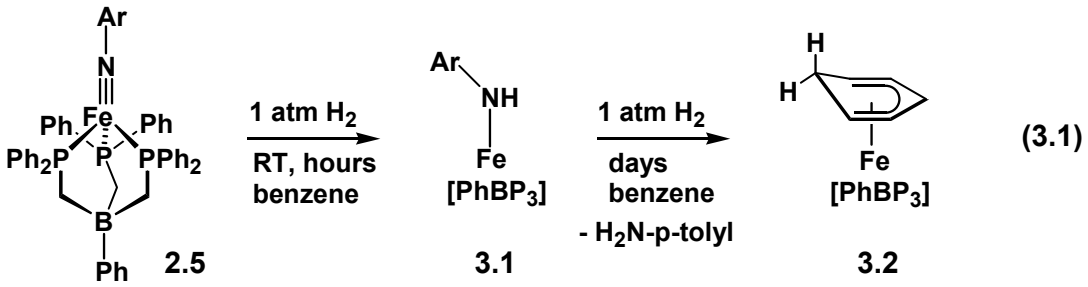

(3.1)

Anilide **3.1** features a weak N-H vibration at 3326 cm^{-1} (Nujol), a temperature-independent magnetic moment of 5.20 μ_B (SQUID, S = 2),[8] and relatively intense charge-transfer bands (450 nm, 3400 M^{-1} cm^{-1}; 547 nm, 3000 M^{-1} cm^{-1}). The solid-state structure of **3.1** (Figure 3.1) is related to that of **2.5** by the addition of a single H-atom at nitrogen. Although both **2.5** and **3.1** are 4-coordinate and pseudotetrahedral, **2.5** features an Fe-N bond distance (1.913(2) Å) and an Fe-N-C bond angle (127.4(2)°) very different from **2.5** (Fe-N = 1.6578(2) Å; Fe-N-C = 169.96(2)°).[4a] Of additional note are the Fe-P bond distances, which are appreciably expanded in the structure of **3.1** (Fe-P_{avg} for **2.5** = 2.24 Å; Fe-P_{avg} for **3.1** = 2.42 Å). These structural differences reflect the low- versus high-spin

configurations of **2.5** and **3.1**, respectively, in addition to the diminished Fe-N π-bond character of **3.1** by comparison to **2.5**.

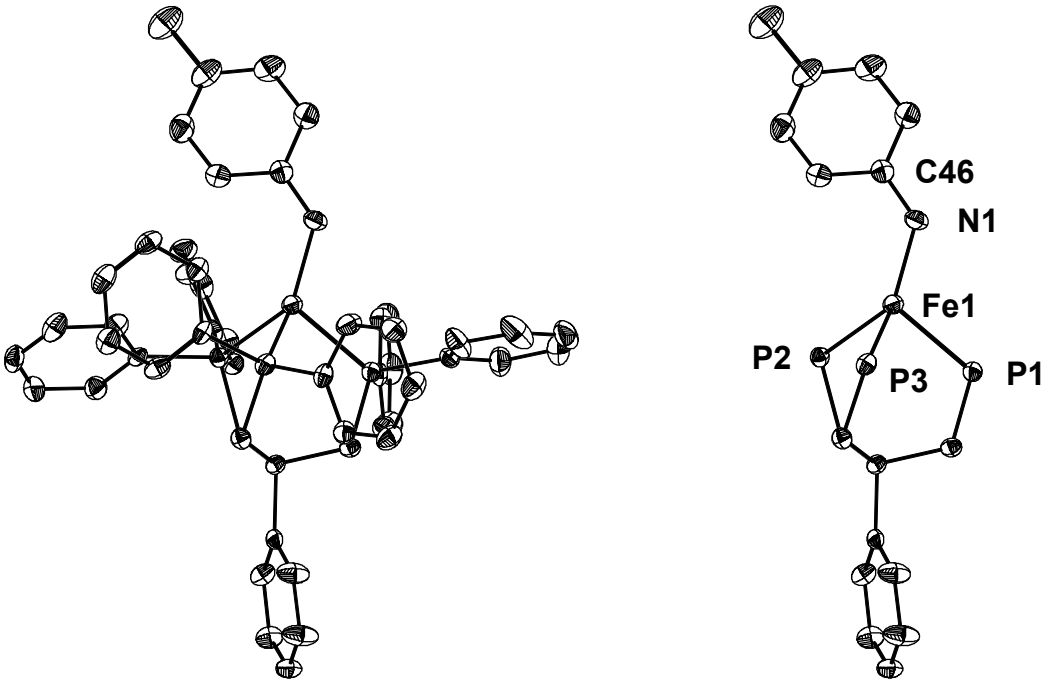

Figure 3.1. 50% thermal ellipsoid representation of [$PhBP_3$]Fe(N(H)-*p*-tolyl) (**3.1**). For the image on the right, all phosphino phenyl groups have been removed for clarity. For both images, all hydrogen atoms have been removed for clarity. Selected bond lengths (Å) and angles (°): Fe1-N1, 1.9132(18); Fe1-P1, 2.3928(7); Fe1-P2, 2.4520(7); Fe1-P3, 2.4267(7); Fe1-N1-C46, 127.44(16); P1-Fe1-P2, 90.29(2); P1-Fe1-P3, 94.44(2); P2-Fe1-P3, 92.64(2); N1-Fe1-P1, 114.15(6); N1-Fe1-P2, 129.34(6); N1-Fe-P3, 126.19(6).

Prolonged monitoring of the hydrogenation of **2.5** in C_6D_6 over a period of days establishes a new diamagnetic product (^{31}P NMR: 52 ppm (s)) and the release of H_2N-*p*-tolyl (40% after 3 days). In a preparative-scale reaction, imide **2.5** was exposed to an atmosphere of H_2 in benzene for 3 days in a sealed reaction flask. Extraction of the crude

solids into diethyl ether left behind the diamagnetic species as a bright orange powder in 25% yield. XRD analysis of a single crystal confirmed it to be the cyclohexadienyl complex [$PhBP_3$]Fe(η^5-cyclohexadienyl) (**3.2**) (Figure 3.2). Complex **3.1** was then isolated in 60% yield from the ethereal extract by crystallization. The combined isolated yield of **3.1** and **3.2** accounted for 85% of the total iron content of the reaction. Similar yields were provided by *in situ* monitoring and integration of ^{1}H NMR spectra of sealed

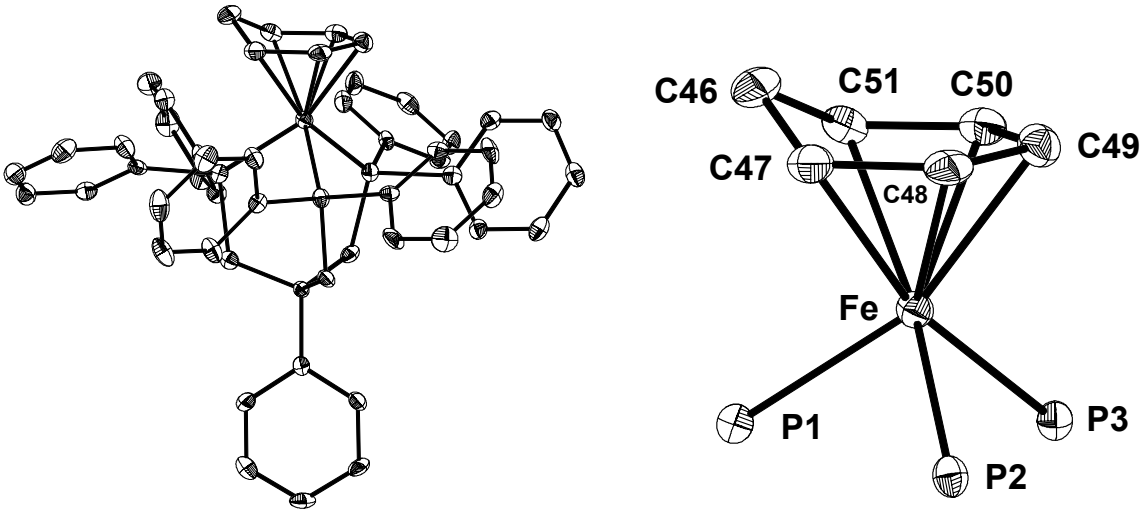

Figure 3.2. 50% thermal ellipsoid representation of [$PhBP_3$]Fe(η^5-cyclohexadienyl) (**3.2**). For the image on the right, only the L_3Fe(η^5-cyclohexadienyl) core is shown. For both images, all hydrogen atoms have been removed for clarity. Selected bond lengths (Å) and angles (°): Fe-P1, 2.2730(10); Fe-P2, 2.2701(10); Fe-P3, 2.2647(9); Fe-C47, 2.213(3); Fe-C48, 2.122(3); Fe-C49, 2.100(3); Fe-C50, 2.098(3); Fe-C51, 2.191(3); P1-Fe-P2, 90.29(2); P1-Fe-P3, 94.44(2); P2-Fe-P3, 92.64(2); C46-C47, 1.477(4); C47-C48, 1.394(4); C48-C49, 1.415(4); C49-C50; 1.410(4); C50-C51, 1.385(4); C51-C46, 1.493(4); P1-Fe-P2, 90.40(3); P1-Fe-P3, 90.92(4); P2-Fe-P3, 88.17(3); C46-C47-C48, 120.5(3); C50-C51-C46, 119.5(3); C47-C46-C51, 104.4(3).

NMR tube experiments after 3 days. Ill-defined paramagnetic resonances indicative of at least one side product account for the remaining iron material (~ 15%) in these sealed-tube experiments. We suspect that the side-product(s) arise from the kinetically competitive degradation of **3.1** during the course of the reaction. As a control experiment, it is noted that the storage of **3.1** in benzene under N_2 leads to some degradation after 3 days but does not produce **3.2**.[9]

To ensure that the H-atoms being delivered to both benzene and the imide functionality arise from H_2, the hydrogenation of **2.5** by D_2 in C_6D_6 was examined. The consumption of **2.5** proceeds in this case much more slowly ($k_{rel} = k(H_2)/k(D_2) = 5.6$; Figure 3.3), and the product yields after 3 days are consequently much lower. The overall reaction is moreover less clean than for the case of H_2 due to the increased role of kinetically competitive side reactions given the longer reaction time. Nonetheless, the

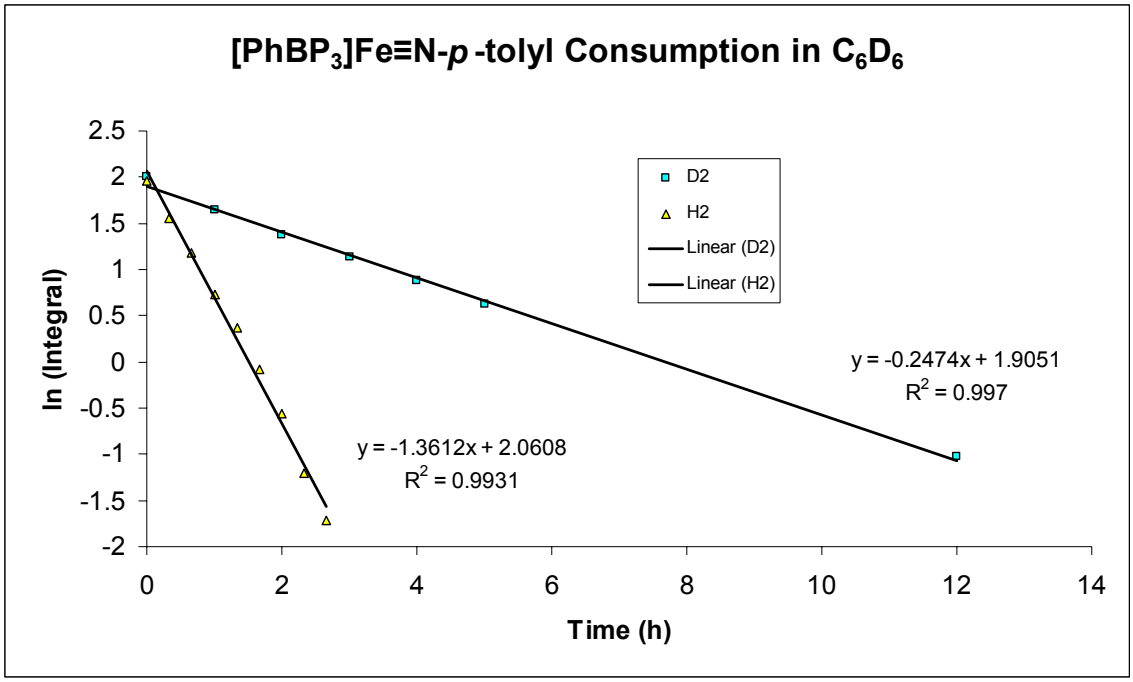

Figure 3.3. Kinetic data for the consumption of **2.5** in C_6D_6 with H_2 (yellow triangles) and D_2 (turquoise squares).

expected products [PhBP$_3$]Fe(N(D)-*p*-tolyl) (**3.1b**), [PhBP$_3$]Fe(η^5-cyclohexadienyl-d_7) (**3.2b**), and D_2N-*p*-tolyl can be identified. Compound **3.1b** is identified on the basis of its ^{1}H NMR resonances and the isotopically shifted N-D stretch in its IR spectrum (Nujol: ν_{ND} = 2462 cm^{-1} (w)). Diamagnetic **3.2b** is assigned from its ^{31}P and ^{1}H NMR spectra. In particular, no cyclohexadienyl ring resonances are present in its ^{1}H NMR spectrum due to complete deuteration. Compound **3.2b** also exhibits the expected ES-MS molecular ion peak at 828 *m*/*z*. The organic byproduct, D_2N-*p*-tolyl, is identified by GC-MS as the only amine-containing product of the reaction.

The reduction of **2.5** to anilide **3.1** and then to **3.2** appears to proceed in a stepwise fashion (Equation 3.1). The detailed mechanism by which these steps occur is clearly of interest but somewhat difficult to unravel due to the paramagnetic nature of **2.5** and **3.1**, in addition to the presence of at least one paramagnetic side product(s) that is formed during the course of the reaction. A reasonable mechanistic outline to suggest is as follows: The first step (**2.5** + 1/2 H_2 $\rightarrow$ **3.1**) involves the addition of H_2 to **2.5** to generate an unobservable species "[PhBP$_3$]Fe^{III}(H)(NHAr)," which, if formed, must bimolecularly release H_2 to provide observable **3.1**. A second addition of H_2 would occur at **3.1** to generate an unobservable "Fe^{II}-H" source (with loss of H_2N-*p*-tolyl) that adds to benzene via insertion.[10,11] Evidence consistent with a reactive "Fe^{II}-H" intermediate comes from the following set of observations: First, the incubation of **3.1** under an atmosphere of H_2 at 25 °C in C_6D_6 slowly generates **3.2** (30% after 3 days) with concomitant evolution of H_2N-*p*-tolyl (50% after 3 days). Second, the addition of $KHBEt_3$ to a benzene solution of [PhBP$_3$]Fe^{II}Cl generates **3.2** in high yield (77% isolated). Moreover, when this latter reaction is carried out in THF rather than benzene a

new and diamagnetic species is generated that can be assigned as the complex $[PhBP_3]Fe^{II}(HBEt_3)$ (**3.3**) on the basis of its solution IR and NMR data in THF (ν_{BH} = 2448 cm^{-1}; ^{31}P NMR: δ 55 ppm (br s); ^{11}B NMR: δ 25.5 ppm (br s, H*B*Et_3), -12.8 ppm (s, Ph*B*$(CH_2PPh_2)_3^-$)). Although crystals of thermally sensitive **3.3** were never obtained,[12] the structurally related complex, $[PhBP_3]Fe(BH_4)$ (**3.4**), was synthesized and fully characterized. The solid-state structure of the latter (Figure 3.4) is consistent with an η^3-borohydride adduct,[13,14] while spectroscopic data is similar to that obtained for **3.3** (ν_{BH} = 2603, 2575 cm^{-1}; ^{31}P NMR: δ 76.2 ppm (s); ^{11}B NMR: δ 22.4 ppm (br s, *B*H_4), -12.9 ppm (s, Ph*B*$(CH_2PPh_2)_3^-$)).

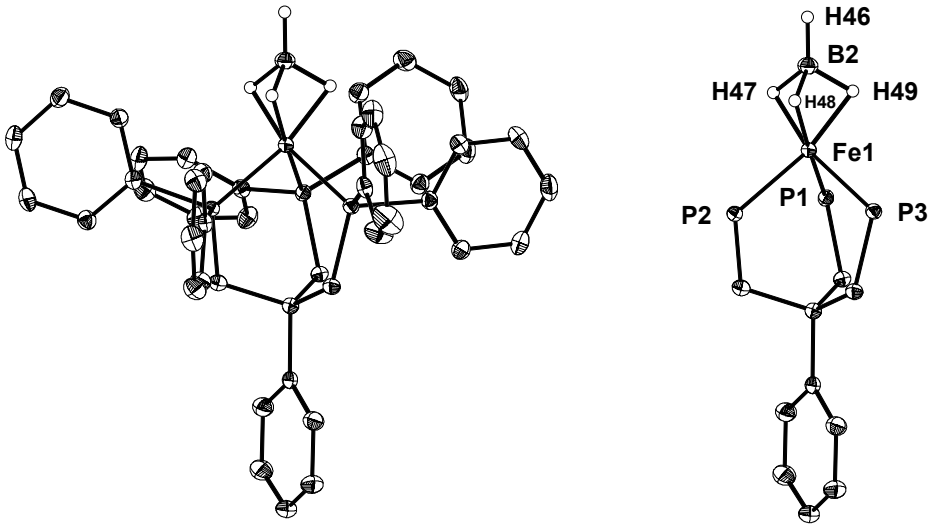

Figure 3.4. 50% thermal ellipsoid representation of $[PhBP_3]Fe(BH_4)$ (**3.4**). For the image on the right, all phosphino phenyl groups have been removed for clarity. For both images, all hydrogen atoms have been removed for clarity. Selected bond lengths (Å) and angles (°): Fe1-B2, 1.8550(15); Fe1-P1, 2.2119(4); Fe1-P2, 2.2088(4); Fe1-P3, 2.1977(4); Fe-H47, 1.570(17); Fe1-H48, 1.615(15); Fe1-H49, 1.612(15); P1-Fe1-P3, 89.53 (2); P2-Fe1-P3, 89.03(2); P1-Fe1-P2, 92.06(2).

Most importantly, complex **3.3** serves as a "[$PhBP_3$]Fe^{II}-H" equivalent and is instantly converted to **3.2** with loss of BEt_3 upon addition of benzene to a THF solution. We also note that the hydrogenation of **2.5** in CD_2Cl_2 generates H_2N-*p*-tolyl and the chloride complex [$PhBP_3$]$Fe^{II}Cl$. Reactive metal hydrides are known to exchange with halocarbons,[15] and it is reasonable to expect that a "[$PhBP_3$]Fe^{II}-H" intermediate might behave similarly.

Whereas iron cyclohexadienyl complexes structurally related to **3.2** are known,[16,17,18] their formation from the insertion of benzene into a reactive Fe-H bond is, to our knowledge, unprecedented. A curious reactivity comparison to note in this context concerns Holland's 4-coordinate iron hydride dimer $\{LFe^{II}H\}_2$, in which L represents a bulky β-diketiminate ligand.[7] This low-coordinate hydride system is isolable and, while reactive toward certain unsaturated substrates (e.g., azobenzene), appears to be stable in aromatic solvents such as benzene.

3.3 Conclusions

In summary, the low-spin iron(III) imide **2.5** undergoes partial and then complete hydrogenation under ambient conditions to release aniline in what appears to be a well-defined, stepwise process. We can directly observe the intermediate Fe(II) anilido species, **3.1**, and have provided evidence for the subsequent intermediacy of a reactive Fe^{II}-H species that is trapped by benzene solvent to provide **3.2**. Interesting mechanistic issues remain to be resolved and are currently under investigation.

3.4 Experimental Section

3.4.1 General Considerations

General considerations are outlined in Section 2.5.1. ^{11}B NMR data was acquired on a JOEL 400 MHz spectrometer and chemical shifts were referenced to neat $BF_3 \cdot OEt_2$ at δ 0 ppm. GC-MS data were obtained by injecting benzene solutions into an Agilent 6890 GC equipped with an Agilent 5973 mass selective detector (EI). IR samples were prepared as either a Nujol mull on CaF_2 plates or as a solution in a sealed cell with KBr plates. Deuterated methylene chloride was purchased from Cambridge Isotope Laboratories, Inc. and was degassed and dried over activated 3 Å molecular sieves prior to use.

3.4.2 Magnetic Measurements

SQUID data for anilide **3.1** was acquired from 2–250 K as outlined in Section 2.5.2, and the corresponding data are shown below.

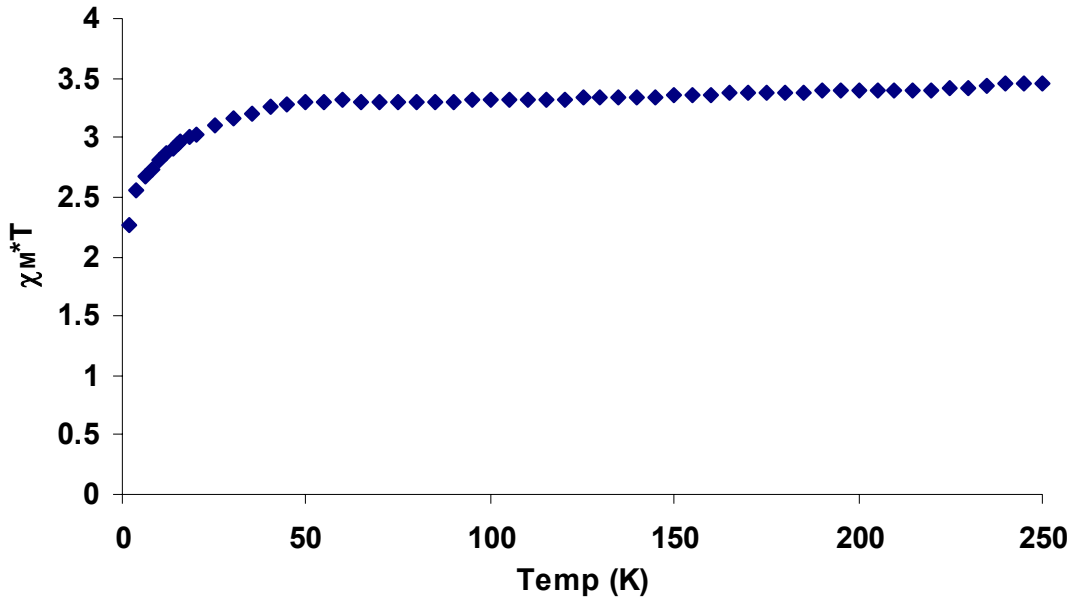

Figure 3.5. Plot of χ_M*T vs. T for [$PhBP_3$]Fe(N(H)-*p*-tolyl) (**3.1**).

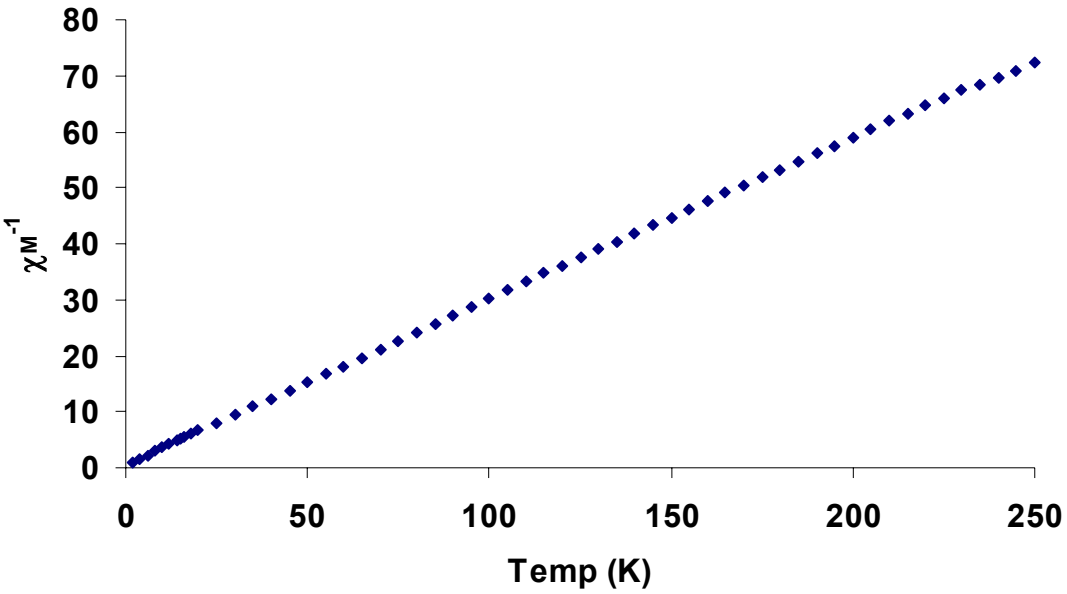

Figure 3.6. Plot of χ_M^{-1} vs. T for [$PhBP_3$]Fe(N(H)-*p*-tolyl) (**3.1**).

3.4.3 Starting Materials and Reagents

Chloride **2.1** and imide **2.5** were prepared according to literature procedures.[4a] [Na][BH_4] and [K][$HBEt_3$] (1.0 M in THF) were obtained from Aldrich. The former was dried overnight under reduced pressure at 150 °C while the latter was used as received. [Li][N(H)-*p*-tolyl] was prepared upon the addition of one equivalent of ^{n}BuLi to *p*-toluidine in petroleum ether. The resulting solid was isolated and dried under reduced pressure. Cylinders of hydrogen and deuterium gas were obtained from Air Liquide and Cambridge Isotope Laboratories, respectively, and used as received.

3.4.4 Synthesis of Compounds

Synthesis of [$PhBP_3$]Fe(N(H)-*p*-tolyl), 3.1: Chloride **2.1** (0.372 g, 0.479 mmol) was added to benzene (10 mL) with stirring. A benzene slurry (2 mL) of [Li][N(H)-*p*-tolyl] (0.0542 g, 0.479 mmol) was then added dropwise at room temperature, which

resulted in a color change from yellow to opaque red/purple. After stirring for two hours the reaction was filtered over celite and volatiles were removed under reduced pressure. The crude solids were then washed with petroleum ether (3 x 20 mL) and dried to afford a dark powder. A crude ^{1}H NMR spectrum of the product demonstrated the presence of **3.1** along with minor paramagnetic impurities. The majority of the impurities were removed by precipitation upon the addition of petroleum ether into a benzene solution. After filtration over Celite the filtrate was chilled to -35 ^{o}C for three days to precipitate 0.194 g (48%) of a dark solid that was predominantly **3.1** but still contaminated by trace impurities; a crystal suitable for X-ray diffraction analysis was collected from the side of the chilled vial. Subsequent vapor diffusion of petroleum ether into a toluene solution of the nearly pure sample of **3.1** provided solids of high enough purity to provide satisfactory combustion analysis. Compound **3.1** was stored at -35 ^{o}C as it degraded over a period of days at room temperature as both a solid and as a benzene solution. ^{1}H NMR (C_6D_6, 300 MHz): δ 139.3 (s); 75.7 (s); 38.3 (s); 18.8 (s); 17.6 (s); 6.63 (s); -11.8 (s); -34.4 (br, s). UV-vis (C_6H_6) λ, nm (ε, M^{-1} cm^{-1}): 450 (3400), 547 (3000). SQUID (solid, average 10 – 250 K): μ_{eff} = 5.20 μ_B. IR (Nujol): 3326 cm^{-1} (w). Anal. Calcd. for $C_{52}H_{49}BFeNP_3$: C, 73.69; H, 5.83; N, 1.65. Found: C, 73.29; H, 5.71; N, 1.60.

Synthesis of [PhBP$_3$]Fe(η^5-cyclohexadienyl), 3.2: Chloride **2.1** (0.050 g, 0.0644 mmol) was added to benzene (3 mL) with stirring. A benzene solution (1 mL) of [K][HBEt$_3$] (71 μL of a 1.0 M solution in THF, 0.0708 mmol) was then added dropwise. After stirring overnight the reaction was filtered over Celite, and volatiles were removed under reduced pressure. The resulting solids were washed with petroleum ether (1 x 5 mL) and dried under reduced pressure to yield **3.2** as an orange powder (0.036 g, 68%).

X-ray quality crystals may be obtained by vapor diffusion of petroleum ether into a THF solution. ^{1}H NMR (C_6D_6, 300 MHz): δ 8.01 (d, *J* = 7.0 Hz, 2H); 7.55 (t, *J* = 7.5 Hz, 2H); 7.34 (t, *J* = 7.5 Hz, 1H); 7.07 (br s, 12H), 6.94 (t, *J* = 7.5 Hz, 6H); 6.77 (t, *J* = 7.5 Hz, 12H); 5.98 (t, *J* = 4.5 Hz, 1H); 5.16 (t, *J* = 4.5 Hz, 2H); 2.66 (m, 2H); 2.29 (m, 2H); 1.65 (br s, 6H). ^{31}P{^{1}H} NMR (C_6D_6, 121.4 MHz): δ 52.0 ppm (s). ES-MS: calcd. for $C_{51}H_{48}BFeP_3$ $[M]^+$ 821 m/z, found $[M]^+$ 821 m/z. Anal. Calcd. for $C_{51}H_{48}BFeP_3$: C, 74.65; H, 5.90. Found: C, 74.32; H, 6.00.

Synthesis of [PhBP$_3$]Fe(HBEt$_3$), 3.3: Chloride **2.1** (0.100 g, 0.129 mmol) was added to Et_2O (10 mL) with stirring. To the stirring slurry of **2.1**, an ethereal solution (2 mL) of [K][HBEt$_3$] (129 μL of a 1 M solution in THF, 0.129 mmol) was added dropwise over a period of 5 minutes. By the time the addition was complete the reaction was midnight blue in color and precipitates were evident. After stirring at room temperature for 20 minutes, the crude reaction was filtered over Celite and the filtrate was cooled to -35 ^{o}C overnight. Approximately 0.060 g (55%) of midnight blue solid was isolated and dried under reduced pressure. Attempts to obtain crystals suitable for an X-ray diffraction experiment have been unsuccessful. The inability to obtain a satisfactory combustion analysis for **3.3** is presumably the result of its thermal instability. ^{1}H NMR (THF-d_8, 300 MHz): δ 7.61 (d, *J* = 7.2 Hz, 2H); 7.27 (br s, 12H); 7.15 (t, *J* = 7.2 Hz, 6H); 7.02 (m, 14H); 6.88 (t, *J* = 7.2 Hz, 1H); 1.44 (br d, *J* = 10.8 Hz, 6H); 0.91 (br s, 6H); 0.68 (t, *J* = 6.6 Hz, 9H). The hydride resonance was not located in the ^{1}H NMR spectrum. ^{31}P{^{1}H} NMR (THF-d_8, 121.4 MHz): δ 55.0 ppm (br s). ^{11}B{^{1}H} NMR (THF-d_8, 128.3 MHz): δ 25.5 ppm (br s, H*B*Et$_3$); -12.8 ppm (s, Ph*B*(CH$_2$PPh$_2$)$_3^-$). IR (KBr/THF): ν_{BH} = 2448 cm^{-1} (br m).

Synthesis of [PhBP$_3$]Fe(BH$_4$), 3.4: Chloride **2.1** (0.100 g, 0.129 mmol) was dissolved in THF (10 mL) with stirring. Solid [Na][BH$_4$] (0.146 g, 3.86 mmol) was added in one portion, which resulted in a color change from yellow to red after stirring overnight. Volatiles were then removed under reduced pressure. The resulting crude solids were extracted with benzene (5 mL), filtered over celite, and lyophilized to yield **3.4** as a red solid (0.92 g, 95%). ^{1}H NMR (300 MHz, C_6D_6): δ 8.10 (d, J = 7.5 Hz, 2H); 7.69 (t, J = 7.5 Hz, 2H); 7.49 (br s, 12H); 7.45 (overlaps with resonance at 7.49 ppm, t, J = 7.5 Hz, 1H); 6.72 (m, 18 H); 1.54 (s, 6H); -11.8 (br s, 4H). ^{31}P{^{1}H} NMR (THF-d_8, 121.4 MHz): δ 76 (br s). ^{11}B{^{1}H} NMR (THF-d_8, 128.3 MHz): δ 22.2 ppm (br s, *B*H$_4$); -12.9 ppm (s, Ph*B*(CH$_2$PPh$_2$)$_3^-$). IR (KBr/C_6H_6): ν_{BH} = 2575 cm^{-1} (m) with a shoulder at 2603 cm^{-1} (m). Anal. Calcd. for $C_{45}H_{45}B_2FeP_3$: C, 71.47; H, 6.00. Found: C, 71.07; H, 6.09.

Reaction of [PhBP$_3$]Fe≡N-*p*-tolyl with H$_2$: Imide **2.5** (0.506 g, 0.598 mmol) was dissolved in benzene (30 mL) and loaded into a 250 mL sealable flask equipped with a stir bar. The flask was evacuated, flushed with 1 atm of H_2, and sealed with a Teflon stopcock. After stirring at room temperature for 3 days, volatiles were removed under reduced pressure, and the resulting solids were stirred in Et_2O (20 mL) for 3 hours. The ethereal suspension was filtered over a sintered glass frit and [PhBP$_3$]Fe(η^5-cyclohexadienyl) (**3.2**) was isolated as an orange solid (0.121 g, 25%) from which X-ray quality crystals were grown via vapor diffusion of petroleum ether into a THF solution. The filtrate was collected and the volatiles were removed under reduced pressure. The resulting dark solids were washed with petroleum ether (3 x 20 mL) and dried to yield 0.205 g of **3.1,** which was slightly contaminated with paramagnetic impurities (^{1}H NMR

spectroscopy). NMR integration of this isolated sample versus an internal ferrocene standard demonstrated that **3.1** had been produced in 60% yield from **2.5** after 3 days.

When the hydrogenation reaction was carried out in C_6D_6, the cyclohexadienyl resonances at δ 5.98, 5.16, and 2.29 ppm disappeared, while the multiplet at δ 2.66 ppm collapsed into a singlet. In C_6D_6 with D_2, the singlet at δ 2.66 ppm disappeared.

Reaction of [PhBP$_3$]Fe≡N-*p*-tolyl with D$_2$: Imide **2.5** (0.0114 g, 0.0135 mmol) was dissolved in benzene-d_6 and loaded into a sealable NMR tube. The NMR tube was then evacuated and flushed with 1 atm of D_2. After 3 days, NMR integration against an internal ferrocene reference demonstrated the following product yields: [PhBP$_3$]Fe(N(D)-*p*-tolyl), 10%; [PhBP$_3$]Fe(η^5-cyclohexadienyl-d_7), 5%; D_2N-*p*-tolyl, 33%. Additionally, no ^{1}H NMR ring resonances were observed for the η^5-cyclohexadienyl-d_7 moiety of [PhBP$_3$]Fe(η^5-cyclohexadienyl-d_7) (**3.2b**). Volatiles were then removed under reduced pressure, and IR analysis confirmed a weak vibration at 2462 cm^{-1} (Nujol) for **3.1b**. ES-MS of the crude solids verified an $[M]^+$ ion at 828 m/z for **3.2b** while GC-MS demonstrated that the only *p*-toluidine in solution was D_2N-*p*-tolyl with a base peak 2 mass units greater than that for H_2N-*p*-tolyl.

Reaction of [PhBP$_3$]Fe≡N-*p*-tolyl with H$_2$ in CD$_2$Cl$_2$: Imide **2.5** (0.0098 g, 0.012 mmol) was dissolved in CD_2Cl_2 and loaded into a sealable NMR tube. The NMR tube was then evacuated and flushed with 1 atm of H_2. After 3 days, NMR integration against an internal ferrocene reference demonstrated the following product yields: [PhBP$_3$]Fe(N(H)-*p*-tolyl), 0%; [PhBP$_3$]FeCl, 30%; H_2N-*p*-tolyl, 80%. Unidentified diamagnetic as well as paramagnetic species were also present in the reaction matrix.

Reaction of [PhBP$_3$]Fe(N(H)-*p*-tolyl) with H$_2$ in C$_6$D$_6$: Anilide **3.1** (0.0083 g, 0.0098 mmol) was dissolved in C_6D_6 and loaded into a sealable NMR tube. The NMR tube was then evacuated and flushed with 1 atm of H_2. After 3 days, NMR integration against an internal ferrocene reference demonstrated the following product yields: [PhBP$_3$]Fe(η^5-cyclohexadienyl-d$_6$) 30%; H_2N-*p*-tolyl, 50%. Unidentified paramagnetic species were also present in the reaction matrix.

Kinetic Analysis for the Consumption of [PhBP$_3$]Fe≡N-*p*-tolyl: Equal volumes of 0.018 M solutions of **2.5** were exposed to 1 atm of either H_2 or D_2 in a sealable NMR tube containing an internal ferrocene standard. The decay of **2.5** was then monitored by ^{1}H NMR spectroscopy for a minimum of 4 half lives (Figure 3.3). Analysis of this data provided a kinetic isotope effect (k_H/k_D) of 5.6, with rate constants of $k(H) = 3.85 \times 10^{-4}$ s^{-1} and $k(D) = 6.88 \times 10^{-5}$ s^{-1}**.**

3.4.5 X-ray Experimental Data

Crystallographic procedures are outlined in Section 2.5.8. Crystallographic data are summarized in Table 3.1. For anilide **3.1**, the location of the amide hydrogen atom was calculated. For borohydride adduct **3.4**, the hydride hydrogen atoms were located in the difference map and refined as normal.

Table 3.1. Crystallographic data for [$PhBP_3$]Fe(N(H)-*p*-tolyl), **3.1**; [$PhBP_3$]Fe(η^5-cyclohexadienyl), **3.2**; and [$PhBP_3$]Fe(BH_4), **3.4**.

	3.1	**3.2**	**3.4**
chemical formula	$C_{52}H_{49}BFeNP_3$	$C_{51}H_{48}BFeP_3$	$C_{45}H_{45}B_2FeP_3$
fw	847.49	820.46	756.19
T (°C)	-177	-177	-177
λ (Å)	0.71073	0.71073	0.71073
a (Å)	10.0087(9)	13.8476(9)	39.226(4)
b (Å)	14.8340(13)	14.5772(9)	13.0057(14)
c (Å)	15.2850(13)	20.3589(13)	16.1408(18)
α (°)	80.110(2)	90	90
β (°)	77.925(2)	90	110.695(4)
γ (°)	87.176(2)	90	90
V (Å^3)	2186.0(3)	4109.6(5)	7703.1(14)
space group	P-1	P2(1)2(1)2(1)	C2/c
Z	2	4	8
D_{calc} (g/cm^3)	1.288	1.326	1.304
μ(cm^{-1})	4.92	5.20	5.48
R1, wR2[a] ($I > 2\sigma(I)$)	0.0489, 0.0813	0.0478, 0.0629	0.0515, 0.0785

[a] $R1 = \Sigma||F_o| - |F_c||/\Sigma|F_o|$, $wR2 = \{\Sigma[w(F_o^2 - F_c^2)^2]/\Sigma[w(F_o^2)^2]\}^{1/2}$

References Cited

[1] Smil, V. *Enriching the Earth*; MIT Press: Cambridge, MA, 2001.

[2] (a) Howard, J. B.; Rees, D. C. *Chem. Rev.* **1996**, *96*, 2965 and references cited therein. (b) Burgess, B. K.; Lowe, D. J. *Chem. Rev.* **1996**, *96*, 2983. (c) Einsle, O.; Tezcan, A.; Andrade, S. L. A.; Schmid, B.; Yoshida, M.; Howard, J. B.; Rees, D. C. *Science* **2002**, *297*, 1696. (d) Thorneley, R. N. F.; Lowe, D. In *Molybdenum Enzymes*; Spiro, T. G., Ed.; Wiley-Interscience: New York, 1985. (e) Sellmann, D.; Sutter, J. *Acc. Chem. Res.* **1997**, *30*, 460. (f) Yandulov, D. V.; Schrock, R. R. *Science* **2003**, *301*, 76. (g) Chatt, J.; Dilworth, J. R.; Richards, R. L. *Chem. Rev*. **1978**, *78*, 589. (h) Richards, R. L. *Coord. Chem. Rev*. **1996**, *154*, 83.

[3] (a) Verma, A. K.; Nazif, T. N.; Achim, C.; Lee, S. C. *J. Am. Chem. Soc.* **2000**, *122*, 11013. (b) Wagner, W. D.; Nakamoto, K. *J. Am. Chem. Soc.* **1989**, *111*, 1590. (c) Meyer, K.; Bill, E.; Mienert, B.; Weyhermuller, T.; Wieghardt, K. *J. Am. Chem. Soc.* **1999**, *121*, 4859. (d) Jensen, M. P.; Mehn, M. P.; Que, L., Jr. *Angew. Chem., Int. Ed*. **2003**, *42*, 4357.

[4] (a) Brown, S. D.; Betley, T. A.; Peters, J. C. *J. Am. Chem. Soc.* **2003**, *125*, 322. (b) Jenkins, D. M.; Betley, T. A.; Peters, J. C. *J. Am. Chem. Soc.* **2002**, *124*, 11238. (c) Betley, T. A.; Peters, J. C. *J. Am. Chem. Soc.* **2003**, *125*, 10782.

[5] Cummins, C. C.; Baxter, S. M.; Wolczanski, P. T. *J. Am. Chem. Soc.* **1988**, *110*, 8731.

[6] For recent examples of terminal imide H_2 chemistry, see: (a) Schmidt, J. A. R.; Arnold, J. *Organometallics* **2002**, *21*, 3426. (b) Burckhardt, U.; Casty, G. L.; Gavenonis, J.; Tilley, T. D. *Organometallics* **2002**, *21*, 3108. (c) Cameron, T. M.; Ortiz, C. G.; Ghiviriga, I.; Abboud, K. A.; Boncella, J. M. *J. Am. Chem. Soc.* **2002**, *124*, 922.

[7] Anilido complexes of divalent iron have been reported recently from direct amination of an auxiliary ligand (see reference 3d) and by thermal degradation of an intermediate hydrazido complex of iron(II). See: Smith, J. M.; Lachicotte, R. J.; Holland, P. L. *J. Am. Chem. Soc*. **2003**, *125*, 15752.

[8] See Section 3.4.2 for the SQUID magnetization data obtained for **3.1**.

[9] While **3.1** can be isolated and thoroughly characterized, including a satisfactory combustion analysis, its ^{1}H NMR spectra invariably show minor impurities because of its tendency to slowly degrade upon dissolution.

[10] Tilley has observed the intramolecular hydrogenation of an aromatic ring upon exposure of a d^0 tantalum imide to hydrogen. This process is believed to occur via an intermediate hydride. See: Gavenonis, J.; Tilley, T. D. *J. Am. Chem. Soc.* **2002**, *124*, 8536.

[11] $[PhBP^{iPr}_3]Fe\text{-}H_x$ species have been isolated and characterized. See: Daida, E. J.; Peters, J. C. *Inorg. Chem.* **2004,** *43,* 7474.

[12] For an example of a structurally characterized η^3-superhydride adduct see: Basuli, F.; Tomaszewski, J.; Huffman, J. C.; Mindiola, D. J. *Organometallics* **2003,** *22,* 4705.

[13] The structurally related compound (triphos)Fe(H)(η^2-BH_4) has been reported. See: (a) Ghilardi, C. A.; Innocenti, P.; Midollini, S.; Orlandini, A. *J. Chem. Soc., Dalton Trans.* **1985,** 605. (b) Ghilardi, C. A.; Innocenti, P.; Midollini, S.; Orlandini, A. *J. Organomet. Chem.* **1982,** *231,* C78.

[14] For $[Tp^{Me2}]Ni(\eta^3\text{-}BH_4)$ see: Desrochers, P. J.; LeLievre, S.; Johnson, R. J.; Lamb, B. T.; Phelps, A. L.; Cordes, A. W.; Gu, W.; Cramer, S. P. *Inorg. Chem.* **2003,** *42,* 7945.

[15] Kaesz, H. D.; Saillant, R. B. *Chem. Rev.* **1972**, *72*, 231.

[16] See for example: (a) Rigaut, S.; Delville, M. H.; Astruc, D. *J. Am. Chem. Soc.* **1997**, *119*, 11132.(b) Lee, S. S.; Lee, I. S.; Chung, Y. K. *Organometallics* **1996**, *15*, 5428. (c) Meng, W. D.; Stephenson, G. R. *J. Organomet. Chem.* **1989**, *371*, 355. (d) Whitesides, T. H.; Arhart, R. W. *J. Am. Chem. Soc.* **1971**, *93*, 5296.

[17] Turculet, L.; Feldman, J. D.; Tilley, T. D. *Organometallics* **2003**, *22*, 4627.

[18] Metal hydride systems are known to catalyze the conversion of benzene to cyclohexane in the presence of hydrogen. For a recent lead reference, see: Suss-Fink, G.; Faure, M.; Ward, T. R. *Angew. Chem., Int. Ed.* **2002**, *41,* 99.